NIH Public Access
Author Manuscript
J Neurochem. Author manuscript; available in PMC 2013 October 01.

Published in final edited form as:
J Neurochem. 2012 October ; 123(1): 44–59. doi:10.1111/j.1471-4159.2012.07870.x.

NeuroD1 is required for survival of photoreceptors but not pinealocytes: Results from targeted gene deletion studies

Margaret J. Ochocinska[1], **Estela M. Muñoz**[2], **Shobi Veleri**[3], **Joan L. Weller**[1], **Steven L. Coon**[1], **Nikita Pozdeyev**[4], **P. Michael Iuvone**[4], **Sandra Goebbels**[5], **Takahisa Furukawa**[6], and **David C. Klein**[1,*]

[1]Section on Neurendocrinology, Program in Developmental Endocrinology and Genetics, The *Eunice Kennedy Shriver* National Institute of Child Health and Human Development, National Institutes of Health, Bethesda, MD

[2]Inst. of Histology and Embryology, Sch. of Medicine, Natl. Univ. of Cuyo, Natl. Council of Research, Sci. and Technol. (CONICET), ANPCyT, Mendoza, Argentina

[3]Neurobiology-Neurodegeneration and Repair Laboratory, National Eye Institute, National Institutes of Health, Bethesda, MD

[4]Dept. of Ophthalmology and Pharmacol., Emory Univ. Sch. of Med., Atlanta, GA

[5]Dept. of Neurogenetics, Max-Planck-Institute of Exp. Med., Göttingen, Germany

[6]Osaka Biosci. Inst., Osaka, Japan

Abstract

NeuroD1 encodes a basic helix-loop-helix (bHLH) transcription factor involved in the development of neural and endocrine structures, including the retina and pineal gland. To determine the effect of *NeuroD1* knockout in these tissues, a Cre/loxP recombination strategy was used to target a *NeuroD1* floxed gene and generate *NeuroD1* conditional knockout (cKO) mice. Tissue specificity was conferred using Cre recombinase expressed under the control of the promoter of *Crx*, which is selectively expressed in the pineal gland and retina. At two months of age *NeuroD1 cKO* retinas have a dramatic reduction in rod- and cone-driven electroretinograms and contain shortened and disorganized outer segments; by four months *NeuroD1* cKO retinas are devoid of photoreceptors. In contrast, the *NeuroD1* cKO pineal gland appears histologically

Corresponding author: Dr. David Charles Klein, Section on Neuroendocrinology, Program in Developmental Endocrinology and Genetics, The Eunice Kennedy Shriver National Institute of Child Health and Human Development, National Institutes of Health, 49 Convent Drive, Room 6A82, Bethesda, MD 20892-4510, USA, kleind@mail.nih.gov, Phone:301-496-6915, Fax:301-480-3526.
Authors:
Margaret J. Ochocinska, Section on Neuroendocrinology, Program in Developmental Endocrinology and Genetics, Eunice Kennedy Shriver National Institute of Child Health and Human Development, National Institutes of Health, Bethesda, MD, USA.
Estela M. Muñoz, Institute of Histology and Embryology, School of Medicine, National University of Cuyo, National Council of Research, Science and Technology (CONICET), ANPCyT, Mendoza, Argentina.
Shobi Veleri, Neurobiology-Neurodegeneration and Repair Laboratory, National Eye Institute, National Institutes of Health, Bethesda, MD, USA.
Joan L. Weller, Section on Neuroendocrinology, Program in Developmental Endocrinology and Genetics, Eunice Kennedy Shriver National Institute of Child Health and Human Development, National Institutes of Health, Bethesda, MD, USA.
Steven L. Coon, Section on Neuroendocrinology, Program in Developmental Endocrinology and Genetics, Eunice Kennedy Shriver National Institute of Child Health and Human Development, National Institutes of Health, Bethesda, MD, USA.
Nikita Pozdeyev, Deptartment of Ophthalmology and Pharmacology, Emory University School of Medicine, Atlanta, GA, USA.
P. Michael Iuvone, Deptartment of Ophthalmology and Pharmacology, Emory University School of Medicine, Atlanta, GA, USA.
Sandra Goebbels, Deptartment of Neurogenetics, Max-Planck-Institute of Experimental Medicine, Göttingen, Germany.
Takahisa Furukawa, 4th Department, Osaka Bioscience Institute, Osaka, Japan.
David Charles Klein, Section on Neuroendocrinology, Program in Developmental Endocrinology and Genetics, Eunice Kennedy Shriver National Institute of Child Health and Human Development, National Institutes of Health, Bethesda, MD, USA.

Any Conflict of Interest: None

NIH-PA Author Manuscript
NIH-PA Author Manuscript
NIH-PA Author Manuscript

NIH-PA Author Manuscript

NIH-PA Author Manuscript

NIH-PA Author Manuscript

normal. Microarray analysis of two-month-old *NeuroD1 cKO* retina and pineal gland identified a subset of genes that were affected 2- to 100-fold; in addition, a small group of genes exhibit altered differential night/day expression. Included in the down-regulated genes are *Aipl1*, which is necessary to prevent retinal degeneration, and *Ankrd33*, which is selectively expressed in the outer segments. These findings suggest that *NeuroD1* may act through *Aipl1* and other genes to maintain photoreceptor homeostasis.

Keywords

NeuroD1; microarray; retina; pineal gland; gene expression; transcriptome profiling

Introduction

NeuroD1 is a basic helix-loop-helix (bHLH) transcription factor implicated in cell cycle regulation, retinal cell genesis, and neuronal development (Miyata *et al.* 1999, Schwab *et al.* 2000, Lee *et al.* 2000, Cai *et al.* 2000, Liu *et al.* 2000, Cherry *et al.* 2011, Ochocinska & Hitchcock, 2009). In the retina, *NeuroD1* plays a role in terminal photoreceptor differentiation and survival of rod photoreceptors; loss of *NeuroD1* results in progressive photoreceptor degeneration (Morrow *et al.* 1999, Pennesi *et al.* 2003). NeuroD1 also functions in cone photoreceptor patterning and mediates cone-specific expression through the regulation of thyroid hormone receptor β2 expression during development (Liu *et al.* 2008).

NeuroD1 mRNA is also highly abundant in the pineal gland and exhibits a developmental expression pattern similar to that of the retina (Bailey *et al.* 2009, Muñoz *et al.* 2007). This is consistent with the common evolutionary origin of pinealocytes and retinal photoreceptors (Klein 2006, Bailey *et al.* 2009, Donoso *et al.* 1985, Korf *et al.* 1985, Korf *et al.* 1992, Rodrigues *et al.* 1986, Reig *et al.* 1990, Schaad *et al.* 1991, Babila *et al.* 1992, Lolley *et al.* 1992). In contrast to the retina, the pineal gland is a relatively homogeneous structure, composed 95% of pinealocytes, which share some genetic features with photoreceptors. This makes the pineal gland a useful model for understanding elements of cell biology shared by both tissues.

Previous studies directed at understanding the role of NeuroD1 in the mouse retina have used a global knockout strategy that eliminates *NeuroD1* expression in all tissues, including the pancreas and cerebellum (Morrow *et al.* 1999, Liu *et al.* 2008). The majority of these animals die shortly after birth, which limits efforts to study *NeuroD1* function in the adult. Moreover, global knock out of *NeuroD1* allows the possibility that the effects of this manipulation on the retina are mediated by non-retinal and non-pineal tissues.

To obviate this possibility in the current study, a Cre/loxP recombination strategy was used to limit gene deletion to the pineal gland and retina. Cre recombinase was selectively expressed in pinealocytes and retinal cells, including photoreceptors, by placing it under control of the *Crx* promoter, which is selectively expressed in both tissues late in gestation (Omori *et al.* 2012, Rath *et al.* 2006, Furukawa *et al.* 2002). *Crx-cre* mice were crossed with *NeuroD1*$^{flox/flox}$ mice (Goebbels *et al.* 2005) to generate *NeuroD1*$^{flox/flox}$/*Crx-cre*$^{+}$ (cKO) and *NeuroD1*$^{flox/flox}$/*Crx-cre*$^{-}$ control mice. The effects of *NeuroD1* cKO on the retina and pineal gland were monitored histologically by immunofluorescence and transmission electron microscopy, and by microarray-based gene expression profiling. Retinal function was monitored using electroretinography. The findings of these studies are presented below.

NIH-PA Author Manuscript

NIH-PA Author Manuscript

NIH-PA Author Manuscript

Materials and Methods

Animals

All animal experiments and treatments were performed in accordance with the National Institutes of Health Guide for Care and Use of Laboratory Animals and the Animal Research: Reporting In Vivo Experiments (ARRIVE) guidelines. Mice were housed in a 12:12 Light-Dark Cycle with lights on at Zeitgeber time (ZT) 0 and food and water *ad libitum*. Both male and female mice were used for all experiments.

NeuroD1 cKO mice: A colony of mice was established on a C57BL/6J background using a male *NeuroD1*$^{flox/flox}$ animal in which exon 2 of the *NeuroD1* gene, which includes the initiating codon, is flanked by two *lox*P sites (Goebbels *et al.* 2005). These animals were crossed with *Crx-cre* mice (Omori *et al.* 2012), which express Cre recombinase under the control of the 2-kb *Crx* promoter (Furukawa *et al.* 2002). See Fig. 1A and Supporting Information for further details.

Agr2$^{-/-}$ mice: A colony of *Agr2* $^{-/-}$ mice was established by crossing a male Agr2$^{+/-}$ animal (Dr. David J. Erle, University of California, San Francisco) with a C57BL/6J female (Taconic Farms) to generate heterozygous progeny (Lewandoski *et al.* 1997, Park *et al.* 2009). These heterozygous progeny were used to generate *Agr2* $^{-/-}$ (*Agr2* KO) and age-matched wild type littermate control animals. See Supporting Information for further details.

Microarray analysis

Pineal glands and retinas from two-month-old *NeuroD1* cKO and control mice were removed during the day at ZT6 and at night at ZT20; tissue was placed on solid CO_2. Tail samples were collected in parallel for genotype confirmation. See Supporting Information for further details.

Total RNA (~200 ng/pineal gland and 1000 ng/retina) was prepared from pools of six pineal glands or retinas; three pools per organ and per genotype were analyzed at each sampling time. Published methods were used for total RNA isolation, quality control, and cDNA amplification (Rovsing et al, 2011). See Supporting Information for further details. Amplified cDNA was biotinylated using the Encore Biotin Module (NuGEN Technologies, Inc.). Biotinylated cDNA (20 ug) was fragmented and hybridized for 18 h at 45°C to the GeneChip Mouse Genome Array 430 2.0 (Affymetrix, Santa Clara, CA). This GeneChip contained 45,000 probe sets corresponding to 39,000 transcripts and variants from over 34,000 annotated mouse genes. The arrays were stained and washed as described in the Affymetrix protocols.

Data analysis

Affymetrix arrays were scanned using a GeneChip Scanner 3000 (Affymetrix). For each array, the raw signal intensity (.CEL) files were generated and analyzed with Genomatix ChipInspector V2.0 software (Munich, Germany). The following filters were used for all analyses: exhaustive matching, a false discovery rate (FDR) = 0, cut off = 1, region size = 300 bp and a minimum of 4 significant probes. Differences of $p < 0.05$ were considered to be statistically significant. See Supporting Information for further details. The microarray data are available at the NCBI Gene Expression Omnibus (www.ncbi.nlm.nih.gov/projects/geo/GSE35396).

Promoter and transcription factor analyses were done using the following Genomatix Software Suite modules (Munich, Germany): Genes2Promoter, RegionMiner, and MatInspector. Briefly, the results from ChipInspector were loaded into the Genes2Promoter

NIH-PA Author Manuscript

NIH-PA Author Manuscript

NIH-PA Author Manuscript

program to identify networks and pathways. RegionMiner was used to identify transcription factor module enrichment from the list of differentially expressed genes and MatInspector was used to inspect the relevant promoter regions.

Quantitative real time polymerase chain reaction (qRT-PCR)

Twenty differentially expressed transcripts ($p<0.05$) were validated by qRT-PCR using the LightCyclerR 480 Rapid Thermal Cycler System (Roche, Indianapolis, IN). The SPIA-amplified cDNA generated for the Microarrays was used as template for all qRT-PCR experiments. PCR reactions were performed in a 25 μL volume consisting of 0.5 μmol/L primers (Table 1), Real-Time SYBR® Green PCR Master Mix (SuperArray Bioscience, Frederick, MD), and cDNA as per the manufacturer's instructions. Published methods were used for all assays (Muñoz et al., 2007). See Supporting Information for further details.

Immunohistochemistry

All immunohistochemistry protocols were performed as previously described (Ochocinska & Hitchcock, 2009). Sections were stained with the following antisera: mouse monoclonal anti-Rho (Rho 4D2; Dr. Robert Molday, University of British Columbia, Vancouver, Canada) diluted 1:1000; rabbit polyclonal anti-M-opsin and antiS-opsin (Dr. Cheryl Craft, University of Southern California, Los Angeles), diluted 1:1000. Secondary antisera included goat anti-rabbit Alexa Fluor® 488 and goat anti-mouse Alexa Fluor® 555 (Invitrogen, Eugene, OR), diluted 1:200. The stained tissue sections were visualized under a LSM 510 META Laser Scanning Confocal Microscope (Carl Zeiss, Maple Grove, MN). See Supporting Information for further details.

Bromodeoxyuridine (BrdU) labeling

BrdU (Sigma, St. Louis, MO) was injected intraperitoneally (0.1mg BrdU/g body wt) at postnatal day 0 (P0) and at two months of age. The animals were sacrificed 4 hours post-injection. Three animals per genotype were analyzed (cKO, N=3; CON, N=3) at both ages.

Western Blot

Retina tissue was homogenized and 100 μg sample of retinal protein was separated by SDS-polyacrylamide gel electrophoresis (PAGE). Blots were incubated with a 1:5000 dilution of affinity-purified Rho 4D2 antiserum overnight at 4°C, followed by a 1- to 2-hour incubation with secondary Alexa Fluor® 680 goat anti-mouse IgG, diluted 1:15,000. Immunoreactive proteins were detected using the Odyssey Infrared Imaging System (Li-Cor; Lincoln, NE) and analyzed by video densitometry (Lynx software; Applied Imaging, Newcastle-upon-Tyne, UK). For semiquantitative analysis, blots were stripped and reprobed with a monoclonal antibody against beta-actin (Sigma, St. Louis, MO), diluted 1:1000, and Alexa Fluor® 800 goat anti-mouse IgG secondary antibody, diluted 1:5000. See Supporting Information for further details.

Transmission Electron Microscopy

Pineal glands were dissected and fixed (1 h at 4°C in 2.5% glutaraldehyde, made in 0.1M sodium cacodylate buffer, pH 7.4). Eyes were dissected and a slit was made in the superior cornea prior to fixation (2 h at 4°C in fixation mix). After the 2 h primary incubation, the superior cornea was cut away, the lens was removed and fixation was continued at 4°C overnight. Tissues were embedded and polymerized in 100% resin for 18 hours in a lab oven set at 70°C. Thin sections (50nm thick) were cut on a Reichert-Jung Ultracut-E ultramicrotome (Leica, Wetzlar, Germany) and collected on LuxFilm grids (Ted Pella, Inc., Redding, CA, Inc.; 30nm film thickness). The grids were post-stained with uranyl acetate

NIH-PA Author Manuscript

NIH-PA Author Manuscript

NIH-PA Author Manuscript

and lead citrate and examined in a Tecnai G2 transmission electron microscope operating at 80kV (FEI, Hillsboro, OR). See Supporting Information for further details.

Electroretinography

Published methods were used for electroretinography (Pang *et al.* 2005). See Supporting Information for further details.

Statistics

Log_2 transformed microarray data from control and *NeuroD1* cKO groups, at ZT6 and ZT20, were compared using two-way ANOVA on GraphPad Prism V4 (GraphPad software). The statistical significance of the microarray, qRT-PCR, and Western blot results was determined by a Student's two-tailed t-test with Welch's correction (Armitage 2002). ERG results were compared using two-way ANOVA on GraphPad Prism V4 (GraphPad software) with p-values of < 0.05 considered statistically significant.

Results

Morphological studies

The NeuroD1 cKO mouse retina has marked morphological changes—To characterize the retinal morphology of *NeuroD1* cKO mice, retinal sections from three animals per genotype were analyzed (cKO, N=3; CON, N=3). Histological analysis revealed that the outer nuclear layer (ONL) in the *NeuroD1* cKO retina is present at two months of age, although the observed thickness varies (Fig. 1B, middle panels). However, the ONL is absent at four months of age (Fig. 1B, right panels). The inner nuclear layer (INL), inner plexiform layer (IPL), and ganglion cell layer (GCL) are not affected in the *NeuroD1* cKO retina based on histological evaluation via light microscopy (Fig. 1B) and transmission electron microscopy, comparing the cellular structures in all three retinal layers, including the ganglion cell layer, inner nuclear layer, and outer nuclear layer (data not shown). Specifically, we examined the morphology of the cells within the respective layers, the organelles within the cells including mitochondria and endoplasmic reticulum and the relationship between respective cells. Due to the absence of the ONL by four months of age, subsequent evaluation of cone and rod photoreceptors was limited to two-month-old retinas.

Cone receptors were examined using antisera against cell type-specific markers M-opsin (Opn1mw) and S-opsin (Opn1sw). M-opsin antisera labeled the outer segments of medium wavelength cone photoreceptors in control retinas. In contrast, in the cKO retina M-opsin immunoreactivity was nearly undetectable (compare Fig. 2A and Fig. 2B). The expression of M-opsin mRNA, was reduced by 80% in the cKO retina compared to controls (Fig. 2C). S-opsin antisera labeled cone outer segments in two-month-old control and *NeuroD1* cKO retinas. However, the outer segments labeled with S-opsin were disorganized; in addition, the S-opsin protein was also mislocalized to the cell membrane and synapse (compare Fig. 2D and Fig. 2E). The expression level of S-opsin transcript, in the cKO and control retinas was similar (Fig. 2F).

Rods were examined at two months of age using antisera against the rod-specific marker Rho. Retinal sections from three animals per genotype were analyzed (cKO, N=3; CON, N=3). The control retina showed a strong Rho signal (Fig. 2G). In contrast, the *NeuroD1* cKO retina showed a weak Rho signal and the protein appeared to be partially mislocalized to the inner segments (Fig. 2H). The Rho-positive outer segments of the *NeuroD1* cKO retina were also shortened and disorganized compared to the controls (Fig. 2H). The red label in the GCL of control and cKO retinas is consistent with the staining pattern of Müller glia end feet.

NIH-PA Author Manuscript

NIH-PA Author Manuscript

NIH-PA Author Manuscript

The immunohistological findings were confirmed by Western blot, which revealed that Rho protein in the two-month-old *NeuroD1 cKO* retina was significantly reduced relative to control (estimated by dilution analysis to be ~95%), (Fig. 2I). In contrast, Rho mRNA was reduced only 40% (Fig. 2J).

Ultrastructural analysis of retinal degeneration in two-month-old NeuroD1 cKO mice—Ultrastructural evaluation of retinas from conditional *NeuroD1* cKO and control mice was performed using transmission electron microscopy (TEM). Retinal sections from three animals per genotype were analyzed (cKO, N=3; CON, N=3). No change in the inner nuclear layer and ganglion cell layer was apparent at the ultrastructural level (data not shown). In the *NeuroD1* cKO retina, the outer segments were disorganized, shortened in length, and, in some regions, completely absent; the controls, in contrast, showed normal outer segments (compare Fig. 3A and C with Fig. 3B and D). The structural integrity of the outer segment discs appears altered and atypical whorls of membranous material (arrows in Fig. 3D) were present between the outer segments and the retinal pigment epithelium (RPE). This expansion of amorphous membranous material is also illustrated in Fig. 3E and at a higher magnification in Fig. 3F.

Ultrastructural analysis of the pineal gland in two-month-old NeuroD1 cKO mice—To determine if there were any changes in pineal gland morphology between genotypes, pineal gland sections from three animals per genotype were analyzed (cKO, N=3; CON, N=3). In contrast to the striking photoreceptor degeneration phenotype observed in the *NeuroD1* cKO retina, there was no obvious change in the morphology of the pineal gland body in *NeuroD1* cKO compared to control mice at the light microscopy level (Fig. 4A and Fig. 4B). The pineal stalk was shorter and wider in the *NeuroD1* cKO animals compared to controls (compare Fig. 4A with Fig. 4B). However, this observation could not be statistically quantified due to the variability in the pineal stalk morphology, and associated technical limitations.

BrdU was used to label mitotically active cells (Wojtowicz & Kee 2006) with the intention of detecting differences between control and *NeuroD1* cKO animals. Injections were performed at postnatal day zero and at two months of age. Brain sections from three animals per genotype and age group were analyzed (cKO, N=3; CON, N=3). BrdU labeling of the control and cKO pineal stalk at both developmental stages was not different (data not shown). This suggests that the pineal stalk phenotype observed in the *NeuroD1* cKO animals is not associated with a difference in proliferation.

Ultrastructural evaluation of pineal glands from two-month-old *NeuroD1* cKO and control mice was performed using TEM. Pineal gland sections from three animals per genotype were analyzed (cKO, N=3; CON, N=3). The morphology of pinealocytes and blood vessels in both groups was normal (Møller *et al.* 1978), as judged by examination of the relationship of pinealocytes to each other and to vascular elements and the appearance of cellular components including the nucleus, mitochondria, ER, membranes and vesicles(Fig. 4C and 4D).

Gene profiling studies

Deletion of NeuroD1 alters the retinal and pineal transcriptomes—The influence of *NeuroD1* on the retina and pineal gland transcriptomes was assessed by Affymetrix microarray analysis in two-month-old control and *NeuroD1* cKO mice. This revealed that *NeuroD1* transcript abundance was reduced by >20-fold in both the retina and pineal gland, confirming the effectiveness of the KO strategy.

NIH-PA Author Manuscript

NIH-PA Author Manuscript

NIH-PA Author Manuscript

The microarray results identified several potential downstream target genes. In the retina, the expression of 55 genes was reduced >2-fold, including genes linked to transcription, phototransduction, and protein folding (Table 2). The most dramatically down-regulated genes included *Ankrd33/Panky* (7.8-fold), and *Agr2* (7.9-fold), which are associated with retinal transcription (Sanuki *et al.* 2010) and protein folding (Persson *et al.* 2005), respectively. The following phototransduction-linked genes did not decrease more than 2-fold, including *Rho, Gnat1, Rcvrn*, *Sag, Arr3*, *Pde6*, and *Grk1.*

In addition to down-regulated genes, it was observed that some genes were upregulated in the retina. The most highly up-regulated gene in the retina was the T cell marker *Tal2* (11.8-fold); others include *Gfap* (5.4-fold), *Prtg* (5.7-fold), *Edn2* (7.4-fold) and *A2m* (7.6-fold), all of which are associated with the immune response (Bucher *et al.* 2000, Kumar & Shamsuddin 2012, Takahashi *et al.* 2010, Rattner & Nathans 2005, Fan *et al.* 2010).

In the *NeuroD1* cKO pineal gland, the expression of 16 genes was reduced > 2-fold (Table 2), including genes linked to transcription and calcium signaling. The most dramatically down-regulated genes included *Agr2* (2.2-fold), *S100a8* (3.3-fold) and *S100a9* (3.1-fold). The most up-regulated gene in the pineal gland was *Igl-V1* (9.1-fold), a member of the immunoglobulin family linked to the immune response (Das *et al.* 2011).

A set of 32 genes exhibited a night/day difference in expression in the control retina; 10 of these genes were also rhythmic in the *NeuroD1* cKO retina. Eleven genes that were rhythmic in the *NeuroD1* cKO retina did not show daily variations in the control retina at the time points studied (Table 3). In the control pineal gland, a set of 38 genes exhibited differential night/day expression; 28 of these genes also exhibited daily rhythms in the *NeuroD1* cKO pineal gland. In addition, 14 genes were only rhythmic in the *NeuroD1* cKO pineal gland (Table 3).

Microarray gene results were validated by qRT-PCR (Table 2). The transcripts examined were those that were most strongly impacted by the *NeuroD1* deletion. In all cases, the results from qRT-PCR analysis qualitatively confirmed the changes observed. For some transcripts, the differences in expression detected by qRT-PCR were >4-fold greater than those revealed by microarray analysis.

In silico promoter analysis of genes affected in NeuroD1 cKO retina and pineal gland—The list of differentially regulated genes in the *NeuroD1* cKO retina and pineal gland, shown in Table 2, was analyzed using the Genomatix Pathway System (GePS). Transcription factor binding sites were determined using RegionMiner, in Genomatix, which compares the promoter regions of the affected group of genes to promoters from the entire genome (Z-score >2, $p<0.05$). NeuroD1 binding sites were present in the promoters of several photoreceptor transduction genes including *Opn1mw*, *Aipl1*, *Agr2*, and *Ankrd33* in the retina (Fig. 5A) and *S100a8*, *S100a9*, *Per3*, and *Agr2* in the pineal gland (Fig. 5B). NeuroD1 dimerizes with its binding partner E47, a bHLH transcription factor, and forms a heterodimer NeuroD1/E47 to translocate to the nucleus and regulate transcription of target genes (Mehmood *et al.* 2011, Mehmood *et al.* 2009, Longo *et al.* 2008). Promoter analysis of the most affected genes using the MatInspector platform revealed that all of the down-regulated genes in the retina contain potential binding sites for the heterodimer NeuroD1/E47 (Fig. 5A). Only two down-regulated genes in the pineal gland, *i.e. Agr2* and *S100a9*, contain putative binding sites for the NeuroD1/E47 complex (Fig. 5B).

The list of genes with altered rhythmic expression on a night/day basis in the retina and pineal gland (Table 3) were analyzed using Genomatix software. To determine whether there was enrichment in specific transcription factor modules which included the NeuroD1/

NIH-PA Author Manuscript

NIH-PA Author Manuscript

NIH-PA Author Manuscript

E47 binding site we used the transcription factor overrepresentation search in Genomatix. This analysis revealed that several transcription factor modules containing NeuroD1 were overrepresented in the genes with altered rhythms in both the retina and pineal gland with Z-scores > 4.0 (Table S1). The most overrepresented modules included the Krüppel-like transcription factor family in the retina (Z-score = 8.1) and the GATA binding factor family in the pineal gland (Z-score = 5.0).

Electroretinography

Rod and cone ERGs are severely compromised in NeuroD1 cKO mice—The role of NeuroD1 in visual physiology was analyzed in *NeuroD1* cKO mice by electoretinography. Rod- and cone-mediated ERGs were recorded to evaluate retinal function in *NeuroD1* cKO mice. Four animals per genotype were analyzed (cKO, N=4; CON, N=4) at two and at four months of age. At two months of age, cKO mice showed significant reductions in rod-driven ERG responses compared to controls (Fig. 6A and Fig. 6C; *p<0.001). Cone ERG responses in cKO mice were reduced to undetectable levels at two months of age (Fig. 6B and Fig. 6D; *p<0.001). Rod and cone ERG responses in the cKO retina were undetectable at four months of age (data not shown).

Cone and rod ERGs in the Agr2$^{-/-}$ mice are normal—The finding that selective knockout of *NeuroD1* decreases the abundance of *Agr2* transcripts raised the possibility that *Agr2* deletion would cause retinal damage. To test this hypothesis, we examined rod and cone electroretinogram responses in *Agr2*$^{-/-}$ (KO) and control (CON) mice. Four animals per genotype were analyzed (KO, N=4; CON, N=4) at two and four months of age. *Agr2*$^{-/-}$ mice displayed normal rod and cone ERGs at both ages (Fig. 7A and Fig. 7B). Significant differences between the average rod and cone-driven b-wave amplitudes were not detected at these ages (Fig. 7C and Fig. 7D) or at six months of age (data not shown).

Discussion

This is the first report on the effect of tissue-specific *NeuroD1* knockout in the adult mouse retina and pineal gland. Analysis of *NeuroD1* cKO retina and pineal gland revealed a marked reduction in *NeuroD1* transcript and severely compromised photoreceptor function. This confirmed that the targeted knockout strategy was effective and establishes a useful model for studies of *NeuroD1*. The results of this study are discussed below from retinal and pineal perspectives, sequentially.

Role of NeuroD1 in retinal biology

The present study extends our understanding of the sequence of events involved in retinal degeneration induced by *NeuroD1* deletion, which we view as a two stage process (Table 4). The first stage is characterized by marked reduction of photodetection as indicated by electroretinography, by changes in outer segments, and by a profound decrease in Rho. However, at this stage, the photoreceptor cell bodies appear to be histologically intact. In agreement, photodetector marker genes remain strongly expressed including transduction genes (*e.g., Rho, Gnat1, Rcvrn*, *Sag, Arr3*, *Pde6*, and *Grk1*) and transcription factor genes (*e.g., Crx, Nrl, and Otx2*). Moreover, the expression of thousands of other genes is also normal. This supports the interpretation that at this stage the cell bodies are not globally impacted by the loss of *NeuroD1.* However, a notable outstanding change observed is a 95% reduction in Rho. The second stage of photoreceptor deterioration is characterized by absence of photoreceptors, as observed by four months of age.

The contrast between the marked change in ERG and the minor change in gene expression at two months suggests that one or all of the small number of genes that are most affected at

NIH-PA Author Manuscript

NIH-PA Author Manuscript

NIH-PA Author Manuscript

this time play a critical role in the loss of photodetection and in disruption of outer segments without marked destruction of cell bodies. This group includes *Aipl1*, *Ankyrd33/Panky*, and *Agr2.* We suspect that the reduction in expression of one or more of these genes and their encoded proteins is critical for the initial deterioration of outer segments. Furthermore the presence of putative binding sites in the promoters of these affected genes suggests that NeuroD1 acts directly on these genes.

Aipl1 has been linked to Leber's congenital amarousis, one of the earliest onset and the most severe forms of inherited retinopathy in humans (Ramamurthy *et al.* 2004). Experimental deletion of *Aipl1* causes a retinal phenotype remarkably similar to the one described in the present study: compromised ERGs, altered structural integrity of the outer segment and the RPE boundary, and photoreceptor-specific degeneration (Ramamurthy *et al.* 2004, Dyer *et al.* 2004). Hence, the *NeuroD1-Aipl1* link established in this study is of special interest because it raises the possibility that retinal pathologies could reflect a reduction in *NeuroD1*-dependent gene expression, leading to a reduction in *Aipl1* expression, which leads to loss of phototransduction.

A second factor that might contribute to the observed effects of *NeuroD1* cKO is *Ankyrd33/Panky,* which encodes a transcriptional cofactor that suppresses Crx-dependent photoreceptor genes (Sanuki *et al.* 2010). Accordingly, down-regulation of *Ankrd33/Panky* may remove suppression of a gene that has a negative influence on photoreceptor biology. An Ankyrd33/Panky knockout mouse model is not available but our expression data, as well as other gene profiling data, suggest that Ankyrd33 is a good retinal degeneration candidate gene (Geisert *et al.* 2009, Sanuki *et al.* 2010).

Decreased expression of *Agr2* may also contribute to the loss of photoreceptor function through an effect on protein folding. This gene encodes a protein disulfide isomerase (Park *et al.* 2009, Persson *et al.* 2005); members of this family insure proper disulfide bonds are formed in newly synthesized proteins. Proper formation of disulfides is required for normal protein function; an example from the retina literature is Rho (McKibbin *et al.* 2007), misfolding of which prevents membrane insertion and proper function. Accordingly, it is possible that the decrease in Agr2 transcripts contributes to the observed effects because substrates of this enzyme, perhaps Rho, are incorrectly folded. However, the finding that $Agr2^{-/-}$ animals have normal ERG responses and relatively normal photoreceptor morphology indicates that loss of *Agr2* alone does not explain the observed *NeuroD1* cKO phenotype. Accordingly, it seems valuable to consider that *Agr2* might contribute to photoreceptor physiology and that photoreceptor loss in the *NeuroD1 cKO* mouse reflects the impact of the partially reduced expression of it together with that of *Aipl1* and *Ankyrd33/Panky*.

The observations in this study are consistent with the interpretation that the gradual loss of photoreceptor cell bodies may involve an immune response in which the initial deterioration of outer segments leads to destruction of photoreceptor cell bodies (Whitcup *et al.* 1998). This is consistent with the increased expression of genes associated with the immune response including *Gfap*, *Prtg*, *Edn2*, *A2m,* and *Tal2*. The most highly up-regulated (>11-fold) gene is T-cell acute lymphocytic leukemia 2 (*Tal2)*, that encodes a bHLH transcription factor which functions as an oncogene whose activation can lead to T-cell leukemia, a cancer of the immune system (Bucher *et al.* 2000, Xia *et al.* 1994, Wadman *et al.* 1994).

NeuroD1 also plays a role in cone photoreceptor specification via regulation of thyroid hormone receptor beta2 (*TRbeta2*) expression (Liu *et al.* 2008). We found similar effects on cone photoreceptor specification but did not observe a change in expression of *TRbeta2* at two months of age. However, the study by Liu *et al.,* (2008) involved embryonic total

NIH-PA Author Manuscript

NIH-PA Author Manuscript

NIH-PA Author Manuscript

NeuroD1 knockout and evaluated early postnatal retinal explants; in contrast, in the present study *NeuroD1* was deleted late in gestation and adult tissue was evaluated. Therefore, it is possible that the differing results in the two studies reflect differences in the timing of the knockout and in the developmental stages examined.

Role of NeuroD1 in pineal biology

In contrast to the retina, deletion of *NeuroD1* did not cause obvious pineal gland morphological effects, although shorter and wider pineal stalks were consistently observed. Deletion of *NeuroD1* did not affect expression of phototransduction- or melatonin synthesis-related genes in the pineal gland, consistent with previous findings in neonatal mice (Muñoz *et al.* 2007). This suggests that *NeuroD1* is not an essential regulator of the melatonin synthesis pathway, but does not eliminate the possibility that it is involved in modulating other aspects of pineal biology, including transcription and calcium signaling, processes which are linked to *S100a8* and *S100a9* (Ghavami *et al.* 2009); expression of which was suppressed in the *NeuroD1* KO pineal gland.

Comparison of the results of the current study with the previous study on *NeuroD1* deletion in neonatal mice reveals notable differences. Total knockout of *NeuroD1* results in increased expression of *Kif5c* and *Gad1* (Muñoz *et al.* 2007) in the neonatal pineal gland; this was not observed in the current study of the adult pineal gland in which the gene deletion occurs late in gestation, when *Crx* is first expressed. Accordingly the differences may reflect differences in the timing of *NeuroD1* deletion and in the ages studied. It is likewise reasonable to suspect that *NeuroD1* may play different roles during pineal development because *NeuroD1* may control transcription in concert with other factors (Cherry *et al.* 2011); different combinations of which in the neonatal versus the adult pineal gland could have differential effects on gene expression.

Day-night analyses of the mouse pineal transcriptome have been previously published (Rovsing *et al.* 2011). Those analyses revealed significant differences in the abundance of rhythmic genes between species: In contrast to >600 genes found to be rhythmic in the rat pineal gland (Bailey *et al.* 2009), only 51 genes showed a day/night rhythm in 129sv mice (Rovsing *et al.* 2011). We compared the list of 51 genes that were rhythmically expressed in 129sv mice (Rovsing et al., 2011) with the list of 38 genes that were rhythmic in the NeuroD1 control pineal glands, which are on a C57BL/6J background. Of the 51 genes that were rhythmically expressed on a day-night basis in the 129sv control pineal glands only 15 were also rhythmic in the C57BL/6J; these included melatonin and signal transduction genes *Aanat*, *Gng4*, *E2f8*, *Cpm*, *Nr1d1*, and *Nrxn3* (Rovsing et al., 2011). This indicates that there are notable strain differences in rhythmic gene expression in this tissue and perhaps others.

Concluding remarks

The findings of this report confirm that *NeuroD1* is required for photoreceptor function and indicate that it may act through a small set of genes to promote retinal survival, specifically through the maintenance of photoreceptor outer segments, loss of which results in photoreceptor degeneration. NeuroD1 may also play a role in pinealocyte homeostasis. The advances from our study are summarized in Fig. 8, which describes the expression of *NeuroD1* and its downstream targets in the photoreceptor and pinealocyte lineages. The absence of *NeuroD1* and its downstream targets results in deterioration of outer segments and leads to the progressive degeneration of photoreceptor cell bodies (Table 5). The *NeuroD1-Aipl1* link established in this study raises the possibility that retinal pathologies could in part reflect a reduction in *NeuroD1*-dependent gene expression, which in turn could suppress expression of *Aipl1* and other genes required for photoreceptor homeostasis.

NIH-PA Author Manuscript

NIH-PA Author Manuscript

NIH-PA Author Manuscript

Supplementary Material

Refer to Web version on PubMed Central for supplementary material.

Acknowledgments

This research was supported by the Intramural Research Program of the National Institute of Child Health, NIH grants R01EY004864 and P30EY006360, and an unrestricted departmental grant from Research to Prevent Blindness, Inc. (RPB). PMI is a recipient of a Senior Scientific Investigator Award from RPB. We would like to thank members of the Klein laboratory, Dr. Morten Møller and Dr. James Russell for many helpful discussions, Dr. Cheryl Craft for the gift of S-opsin and M-opsin antisera, Dr. Robert Molday for the gift of the Rho (Rho 4D2) antiserum, Dr. David J. Erle for the gift of *Agr2*$^{+/-}$ mice, Chip Dye (NICHD Microscopy and Imaging Core) for his help with transmission electron microscopy, Dr. Anand Swaroop and members of the Neurobiology-Neurodegeneration and Repair Laboratory and Dr. Haohua Qian in the NEI Visual Function Core for assistance with electroretinography, and Daniel Abebe for his veterinary support.

Abbreviations used

bHLH	basic helix-loop-helix
cKO	conditional knockout
CON	control
ZT	Zeitgeber time
BrdU	bromodeoxyuridine
ERG	electroretinogram
ONL	outer nuclear layer
INL	inner nuclear layer
GCL	ganglion cell layer
RPE	retinal pigment epithelium
TEM	transmission electron microscopy
DAPI	4′,6-Diamidino-2-Phenylindole

References

Armitage, P.; Berry, G.; Matthews, JNS. Statistical Methods in Medical Research. 4. Blackwell Science; Oxford: 2002.

Babila T, Schaad NC, Simonds WF, Shinohara T, Klein DC. Development of MEKA (phosducin), G beta, G gamma and S-antigen in the rat pineal gland and retina. Brain Res. 1992; 585:141–148. [PubMed: 1511297]

Bailey MJ, Coon SL, Carter DA, et al. Night/day changes in pineal expression of >600 genes: central role of adrenergic/cAMP signaling. J Biol Chem. 2009; 284:7606–7622. [PubMed: 19103603]

Bucher K, Sofroniew MV, Pannell R, et al. The T cell oncogene Tal2 is necessary for normal development of the mouse brain. Dev Biol. 2000; 227:533–544. [PubMed: 11071772]

Cai L, Morrow EM, Cepko CL. Misexpression of basic helix-loop-helix genes in the murine cerebral cortex affects cell fate choices and neuronal survival. Development. 2000; 127:3021–3030. [PubMed: 10862740]

Cherry TJ, Wang S, Bormuth I, Schwab M, Olson J, Cepko CL. NeuroD factors regulate cell fate and neurite stratification in the developing retina. J Neurosci. 2011; 31:7365–7379. [PubMed: 21593321]

NIH-PA Author Manuscript

NIH-PA Author Manuscript

NIH-PA Author Manuscript

Das S, Hirano M, McCallister C, Tako R, Nikolaidis N. Comparative genomics and evolution of immunoglobulin-encoding loci in tetrapods. Adv Immunol. 2011; 111:143–178. [PubMed: 21970954]

Donoso LA, Merryman CF, Edelberg KE, Naids R, Kalsow C. S-antigen in the developing retina and pineal gland: a monoclonal antibody study. Invest Ophthalmol Vis Sci. 1985; 26:561–567. [PubMed: 3884540]

Dyer MA, Donovan SL, Zhang J, Gray J, Ortiz A, Tenney R, Kong J, Allikmets R, Sohocki MM. Retinal degeneration in Aipl1-deficient mice: a new genetic model of Leber congenital amaurosis. Brain Res Mol Brain Res. 2004; 132:208–220. [PubMed: 15582159]

Fan W, Li X, Wang W, Mo JS, Kaplan H, Cooper NG. Early Involvement of Immune/Inflammatory Response Genes in Retinal Degeneration in DBA/2J Mice. Ophthalmol Eye Dis. 2010; 1:23–41. [PubMed: 20352036]

Furukawa A, Koike C, Lippincott P, Cepko CL, Furukawa T. The mouse Crx 5′-upstream transgene sequence directs cell-specific and developmentally regulated expression in retinal photoreceptor cells. J Neurosci. 2002; 22:1640–1647. [PubMed: 11880494]

Geisert EE, Lu L, Freeman-Anderson NE, Templeton JP, Nassr M, Wang X, Gu W, Jiao Y, Williams RW. Gene expression in the mouse eye: an online resource for genetics using 103 strains of mice. Mol Vis. 2009; 15:1730–1763. [PubMed: 19727342]

Ghavami S, Chitayat S, Hashemi M, Eshraghi M, Chazin WJ, Halayko AJ, Kerkhoff C. S100A8/A9: a Janus-faced molecule in cancer therapy and tumorgenesis. Eur J Pharmacol. 2009; 625:73–83. [PubMed: 19835859]

Goebbels S, Bode U, Pieper A, Funfschilling U, Schwab MH, Nave KA. Cre/loxP-mediated inactivation of the bHLH transcription factor gene NeuroD/BETA2. Genesis. 2005; 42:247–252. [PubMed: 16028233]

Klein DC. Evolution of the vertebrate pineal gland: the AANAT hypothesis. Chronobiol Int. 2006; 23:5–20. [PubMed: 16687276]

Korf HW, Foster RG, Ekstrom P, Schalken JJ. Opsin-like immunoreaction in the retinae and pineal organs of four mammalian species. Cell Tissue Res. 1985; 242:645–648. [PubMed: 2934135]

Korf HW, White BH, Schaad NC, Klein DC. Recoverin in pineal organs and retinae of various vertebrate species including man. Brain Res. 1992; 595:57–66. [PubMed: 1467959]

Kumar A, Shamsuddin N. Retinal Muller glia initiate innate response to infectious stimuli via toll-like receptor signaling. PLoS One. 2012; 7:e29830. [PubMed: 22253793]

Lee JK, Cho JH, Hwang WS, Lee YD, Reu DS, Suh-Kim H. Expression of neuroD/BETA2 in mitotic and postmitotic neuronal cells during the development of nervous system. Dev Dyn. 2000; 217:361–367. [PubMed: 10767080]

Lewandoski M, Meyers EN, Martin GR. Analysis of Fgf8 gene function in vertebrate development. Cold Spring Harb Symp Quant Biol. 1997; 62:159–168. [PubMed: 9598348]

Liu H, Etter P, Hayes S, Jones I, Nelson B, Hartman B, Forrest D, Reh TA. NeuroD1 regulates expression of thyroid hormone receptor 2 and cone opsins in the developing mouse retina. J Neurosci. 2008; 28:749–756. [PubMed: 18199774]

Liu M, Pereira FA, Price SD, et al. Essential role of BETA2/NeuroD1 in development of the vestibular and auditory systems. Genes Dev. 2000; 14:2839–2854. [PubMed: 11090132]

Lolley RN, Craft CM, Lee RH. Photoreceptors of the retina and pinealocytes of the pineal gland share common components of signal transduction. Neurochem Res. 1992; 17:81–89. [PubMed: 1538828]

Longo A, Guanga GP, Rose RB. Crystal structure of E47-NeuroD1/beta2 bHLH domain-DNA complex: heterodimer selectivity and DNA recognition. Biochemistry. 2008; 47:218–229. [PubMed: 18069799]

McKibbin C, Toye AM, Reeves PJ, Khorana HG, Edwards PC, Villa C, Booth PJ. Opsin stability and folding: the role of Cys185 and abnormal disulfide bond formation in the intradiscal domain. J Mol Biol. 2007; 374:1309–1318. [PubMed: 17988684]

Mehmood R, Yasuhara N, Fukumoto M, Oe S, Tachibana T, Yoneda Y. Cross-talk between distinct nuclear import pathways enables efficient nuclear import of E47 in conjunction with its partner transcription factors. Mol Biol Cell. 2011; 22:3715–3724. [PubMed: 21832153]

NIH-PA Author Manuscript

NIH-PA Author Manuscript

NIH-PA Author Manuscript

Mehmood R, Yasuhara N, Oe S, Nagai M, Yoneda Y. Synergistic nuclear import of NeuroD1 and its partner transcription factor, E47, via heterodimerization. Exp Cell Res. 2009; 315:1639–1652. [PubMed: 19272376]

Miyata T, Maeda T, Lee JE. NeuroD is required for differentiation of the granule cells in the cerebellum and hippocampus. Genes Dev. 1999; 13:1647–1652. [PubMed: 10398678]

Møller M, van Deurs B, Westergaard E. Vascular permeability to proteins and peptides in the mouse pineal gland. Cell Tissue Res. 1978; 195:1–15. [PubMed: 737703]

Morrow EM, Furukawa T, Lee JE, Cepko CL. NeuroD regulates multiple functions in the developing neural retina in rodent. Development. 1999; 126:23–36. [PubMed: 9834183]

Muñoz EM, Bailey MJ, Rath MF, Shi Q, Morin F, Coon SL, Møller M, Klein DC. NeuroD1: developmental expression and regulated genes in the rodent pineal gland. J Neurochem. 2007; 102:887–899. [PubMed: 17630985]

Nishida A, Furukawa A, Koike C, Tano Y, Aizawa S, Matsuo I, Furukawa T. Otx2 homeobox gene controls retinal photoreceptor cell fate and pineal gland development. Nat Neurosci. 2003; 6:1255–1263. [PubMed: 14625556]

Ochocinska MJ, Hitchcock PF. NeuroD regulates proliferation of photoreceptor progenitors in the retina of the zebrafish. Mech Dev. 2009; 126:128–141. [PubMed: 19121642]

Omori Y, Araki F, Chaya T, Kajimura N, Irie S, Terada K, Muranishi Y, Tsujii T, Ueno S, Koyasu T, Tamaki Y, Kondo M, Amano S, Furukawa T. Presynaptic dystroglycan-pikachurin complex regulates the proper synaptic connection between retinal photoreceptor and bipolar cells. J Neurosci in press. 2012

Pang JJ, Chang B, Hawes NL, et al. Retinal degeneration 12 (rd12): a new, spontaneously arising mouse model for human Leber congenital amaurosis (LCA). Mol Vis. 2005; 11:152–162. [PubMed: 15765048]

Park SW, Zhen G, Verhaeghe C, Nakagami Y, Nguyenvu LT, Barczak AJ, Killeen N, Erle DJ. The protein disulfide isomerase AGR2 is essential for production of intestinal mucus. Proc Natl Acad Sci U S A. 2009; 106:6950–6955. [PubMed: 19359471]

Pennesi ME, Cho JH, Yang Z, Wu SH, Zhang J, Wu SM, Tsai MJ. BETA2/NeuroD1 null mice: a new model for transcription factor-dependent photoreceptor degeneration. J Neurosci. 2003; 23:453–461. [PubMed: 12533605]

Persson S, Rosenquist M, Knoblach B, Khosravi-Far R, Sommarin M, Michalak M. Diversity of the protein disulfide isomerase family: identification of breast tumor induced Hag2 and Hag3 as novel members of the protein family. Mol Phylogenet Evol. 2005; 36:734–740. [PubMed: 15935701]

Ramamurthy V, Niemi GA, Reh TA, Hurley JB. Leber congenital amaurosis linked to AIPL1: a mouse model reveals destabilization of cGMP phosphodiesterase. Proc Natl Acad Sci U S A. 2004; 101:13897–13902. [PubMed: 15365178]

Rath MF, Munoz E, Ganguly S, Morin F, Shi Q, Klein DC, Møller M. Expression of the Otx2 homeobox gene in the developing mammalian brain: embryonic and adult expression in the pineal gland. J Neurochem. 2006; 97:556–566. [PubMed: 16539656]

Rattner A, Nathans J. The genomic response to retinal disease and injury: evidence for endothelin signaling from photoreceptors to glia. J Neurosci. 2005; 25:4540–4549. [PubMed: 15872101]

Reig JA, Yu L, Klein DC. Pineal transduction. Adrenergic----cyclic AMP-dependent phosphorylation of cytoplasmic 33-kDa protein (MEKA) which binds beta gamma-complex of transducin. J Biol Chem. 1990; 265:5816–5824. [PubMed: 2156830]

Rodrigues MM, Hackett J, Gaskins R, Wiggert B, Lee L, Redmond M, Chader GJ. Interphotoreceptor retinoid-binding protein in retinal rod cells and pineal gland. Invest Ophthalmol Vis Sci. 1986; 27:844–850. [PubMed: 3700035]

Rovsing L, Clokie S, Bustos DM, Rohde K, Coon SL, Litman T, Rath MF, Møller M, Klein DC. Crx broadly modulates the pineal transcriptome. J Neurochem. 2011; 119:262–274. [PubMed: 21797868]

Sanuki R, Omori Y, Koike C, Sato S, Furukawa T. Panky, a novel photoreceptor-specific ankyrin repeat protein, is a transcriptional cofactor that suppresses CRX-regulated photoreceptor genes. FEBS Lett. 2010; 584:753–758. [PubMed: 20026326]

NIH-PA Author Manuscript

NIH-PA Author Manuscript

NIH-PA Author Manuscript

Schaad NC, Shinohara T, Abe T, Klein DC. Photoneural control of the synthesis and phosphorylation of pineal MEKA (phosducin). Endocrinology. 1991; 129:3289–3298. [PubMed: 1659528]

Schwab MH, Bartholomae A, Heimrich B, et al. Neuronal basic helix-loop-helix proteins (NEX and BETA2/Neuro D) regulate terminal granule cell differentiation in the hippocampus. J Neurosci. 2000; 20:3714–3724. [PubMed: 10804213]

Takahashi KF, Kiyoshima T, Kobayashi I, et al. Protogenin, a new member of the immunoglobulin superfamily, is implicated in the development of the mouse lower first molar. BMC Dev Biol. 2010; 10:115. [PubMed: 21108791]

Wadman I, Li J, Bash RO, Forster A, Osada H, Rabbitts TH, Baer R. Specific in vivo association between the bHLH and LIM proteins implicated in human T cell leukemia. EMBO J. 1994; 13:4831–4839. [PubMed: 7957052]

Whitcup SM, Vistica BP, Milam AH, Nussenblatt RB, Gery I. Recoverin-associated retinopathy: a clinically and immunologically distinctive disease. Am J Ophthalmol. 1998; 126:230–237. [PubMed: 9727517]

Wojtowicz JM, Kee N. BrdU assay for neurogenesis in rodents. Nat Protoc. 2006; 1:1399–1405. [PubMed: 17406427]

Xia Y, Hwang LY, Cobb MH, Baer R. Products of the TAL2 oncogene in leukemic T cells: bHLH phosphoproteins with DNA-binding activity. Oncogene. 1994; 9:1437–1446. [PubMed: 8152805]

NIH-PA Author Manuscript
NIH-PA Author Manuscript
NIH-PA Author Manuscript

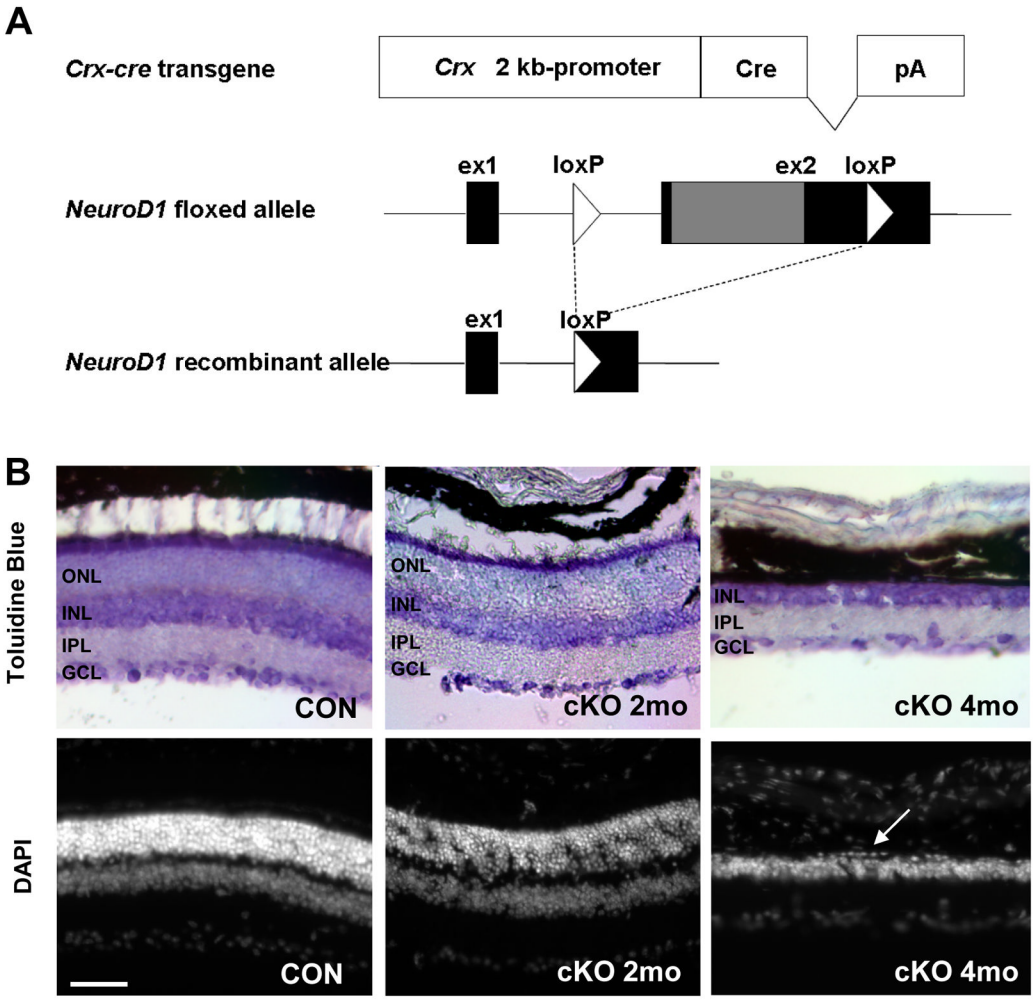

Figure 1. Generation of *NeuroD1* conditional knockout mice

(A) Schematic of constructs. Mice expressing Cre recombinase under the control of the *Crx* 2-kb promoter were crossed with the *NeuroD1*^{flox} mouse line, in which the second exon of the *NeuroD1* gene is flanked by two *lox*P sites. We obtained *NeuroD1*$^{flox/flox}$/*Crx-cre*$^{+}$ mice as *NeuroD1* conditional knockout (cKO) mice by mating *NeuroD1*$^{flox/flox}$ mice with *NeuroD1*$^{+/flox}$/*Crx-cre*$^{+}$ mice. (B) Retina sections from two-month-old control and two- and four-month-old *NeuroD1* cKO mice were stained with toluidine blue (top three panels) and DAPI (bottom three panels). The ONL is present in two-month-old control and *NeuroD1* cKO retinas, respectively (left and middle panels). Histology reveals the absence of the outer nuclear layer (ONL) by four months in *NeuroD1* cKO retinas (arrow, right panel). The inner nuclear layer (INL), inner plexiform layer (IPL), and the ganglion cell layer (GCL) are not affected. Scale bar: 50μm. See Materials and Methods for further details.

NIH-PA Author Manuscript
NIH-PA Author Manuscript
NIH-PA Author Manuscript

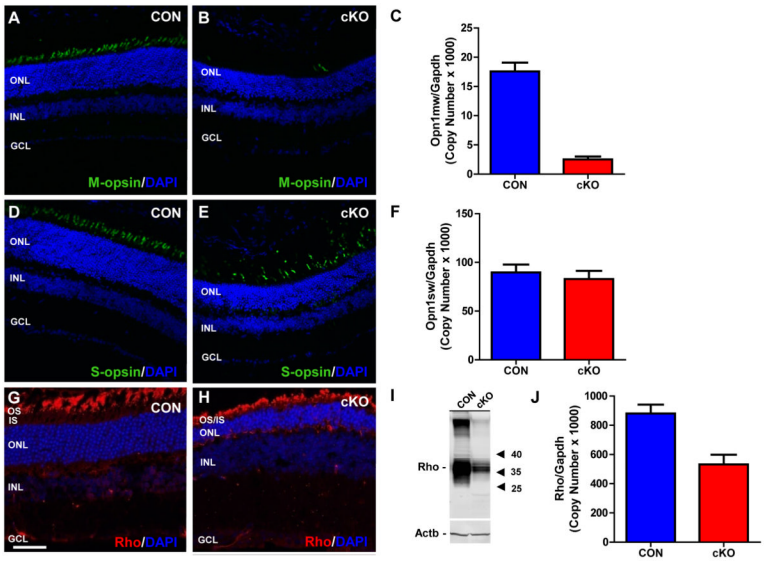

Figure 2. Effect of NeuroD1 conditional knockout on photoreceptors

(A) M-opsin protein is expressed in outer segments of medium wave length cones in control retinas. (B) Conditional knockout of *NeuroD1* results in depletion of medium wave length cones. (C) The expression of M-opsin mRNA is reduced in cKO retinas compared to controls, as shown by qRT-PCR. (D) S-opsin protein is expressed in the outer segments of short wave length cones in control retinas. (E) Conditional knockout of *NeuroD1* results in depletion of short wave length cones. S-opsin protein is also mislocalized to the cell membrane and synapse. (F) There is no change in the expression of S-opsin mRNA in cKO retinas compared to controls, as shown by qRT-PCR. (G) Rho protein is expressed in the outer segments of rod photoreceptors in the control retina. (H) In the cKO retina Rho protein is expressed in both the inner segments and outer segments, which appear shortened compared to controls. (I) Rho protein is decreased 95% in the cKO retina compared to the control retina, as shown by Western blotting using dilution analysis. The lower band is the actin loading control. (J) The expression of Rho mRNA is reduced by ~ 40% in the cKO retinas compared to controls, as shown by qRT-PCR. DAPI (blue); M-opsin (green in panels A and B); S-opsin (green in panels C and D); Rho (red in panels E and F). Scale bar: 50μm. See Materials and Methods for further details.

NIH-PA Author Manuscript
NIH-PA Author Manuscript
NIH-PA Author Manuscript

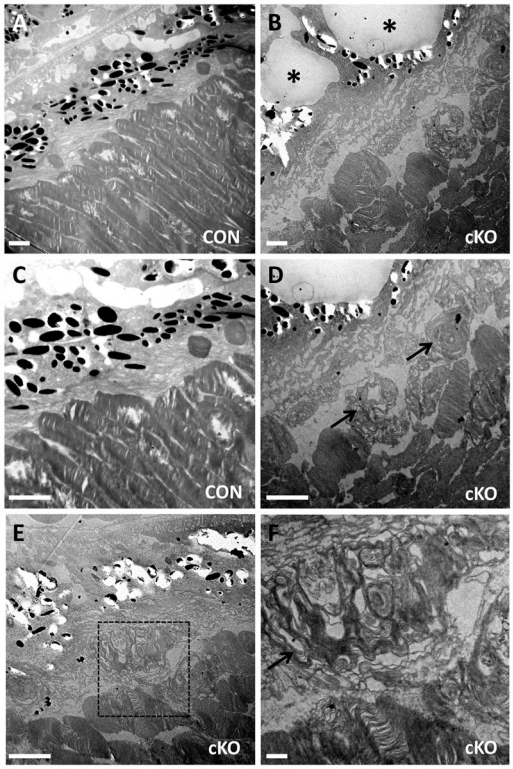

Figure 3. Changes in ultrastructure of *NeuroD1* cKO retina at two months of age

(A and C) Organized outer segments are present in the control retina. Phagosomes can be observed (arrow head) during the disk shedding process. (B and D) The outer segments in the cKO retina are disorganized and form membranous whorls (arrows). Note the absence of phagosomes and disc shedding. The asterisks label large vacuoles indicative of retinal degeneration. (E) Long retinal pigment epithelium processes extend towards the outer segment whorls of the cKO retina. (F) An enlargement of the region framed by the box (dashed line) in panel E emphasizing the amorphous processes in this area (arrows). Scale bars: (A – E) 2 μm, (F) 0.5 μm. See Materials and Methods for further details.

NIH-PA Author Manuscript
NIH-PA Author Manuscript
NIH-PA Author Manuscript

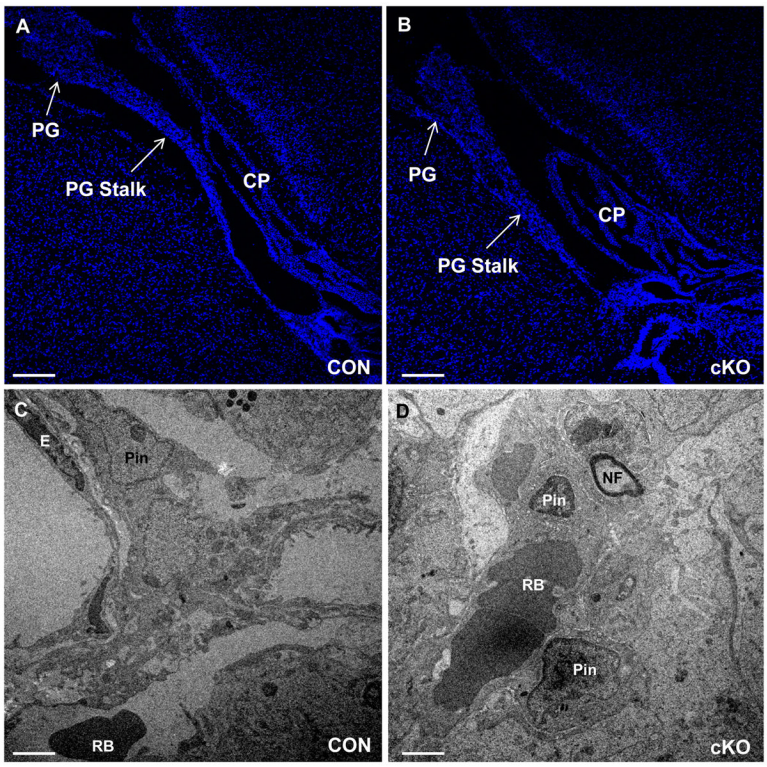

Figure 4. Morphology and ultrastructure of two-month-old *NeuroD1* cKO and control pineal gland

(A and B) DAPI stained (blue) section of brains from two-month-old control and *NeuroD1* cKO mice, respectively, showing the pineal gland and stalk. (C) Control pineal gland with endocrine characteristics including blood vessels and pinealocytes. (D) The *NeuroD1* cKO pineal gland also contains a normal complement of pinealocytes, endothelial cells, red blood cells, and nerve fibers. Scale bar: (A and B) 200 μm, (C and D): 2 μm. PG, pineal gland; Pin, pinealocyte; CP, choroid plexus; E, endothelial cell; RB, red blood cell; NF, nerve fiber. See Materials and Methods for further details.

NIH-PA Author Manuscript
NIH-PA Author Manuscript
NIH-PA Author Manuscript

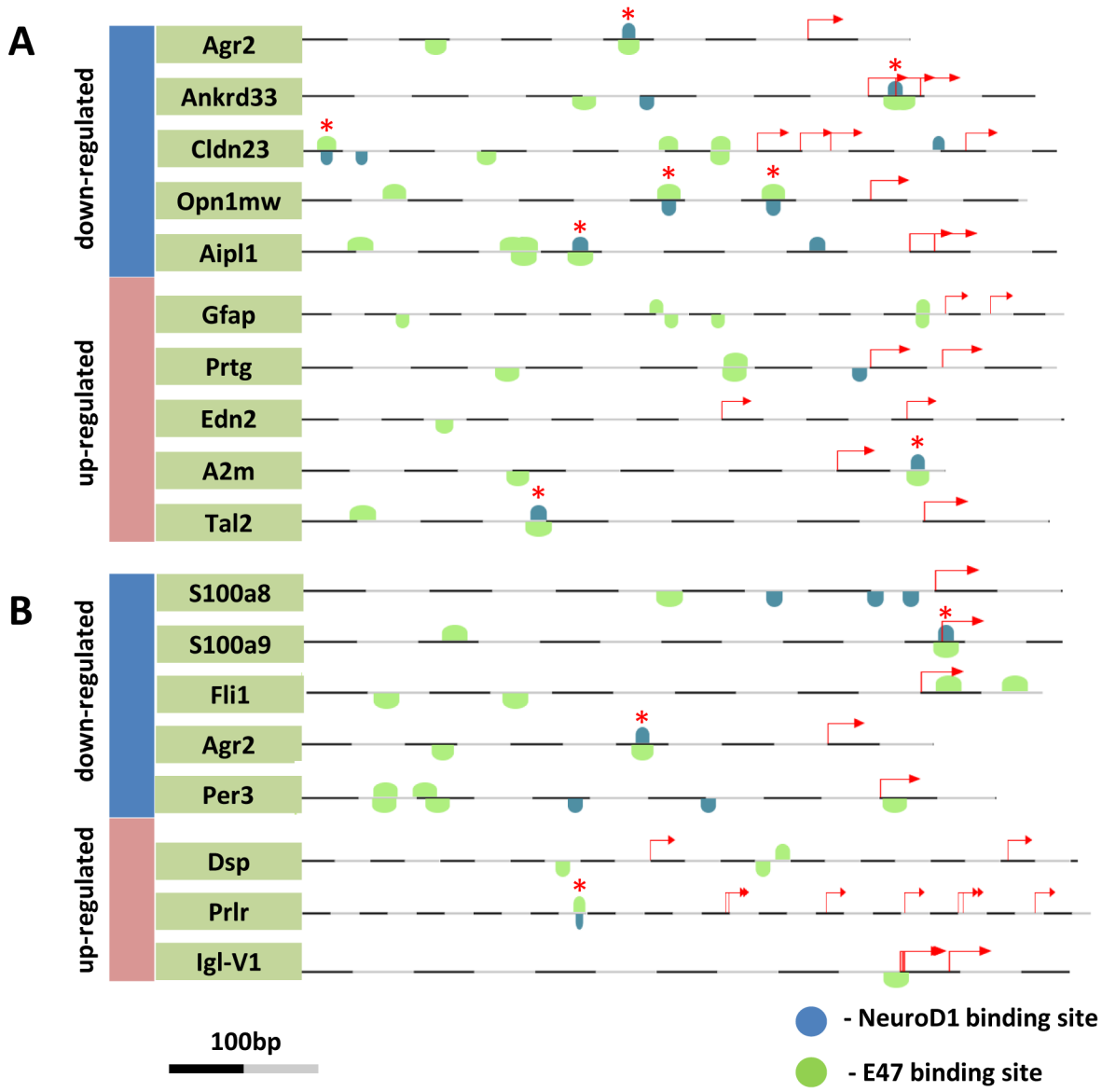

Figure 5. ***In silico*** **Promoter analysis of differentially expressed genes in the** ***NeuroD1*** **cKO retina and pineal gland using Genomatix software**

(A) Promoter analysis of the most affected genes in the cKO retina using the Genomatix MatInspector platform. NeuroD1 binding sites are labeled in blue and E47 binding sites are labeled in green. All of the down-regulated genes identified in the retina contain putative active binding sites for both *NeuroD1* and its partner E47 (red asterisks). Potential DNA binding sites for the heterodimer NeuroD1/E47 are present in two of the five up-regulated genes analyzed, *A2m* and *Tal 2*. (B) The down-regulated genes *Agr2* and *S100a9* in the pineal gland contain putative active binding sites for the heterodimer NeuroD1/E47. *Prlr* gene is the only up-regulated gene with this class of DNA binding site. See Materials and Methods for further details.

NIH-PA Author Manuscript
NIH-PA Author Manuscript
NIH-PA Author Manuscript

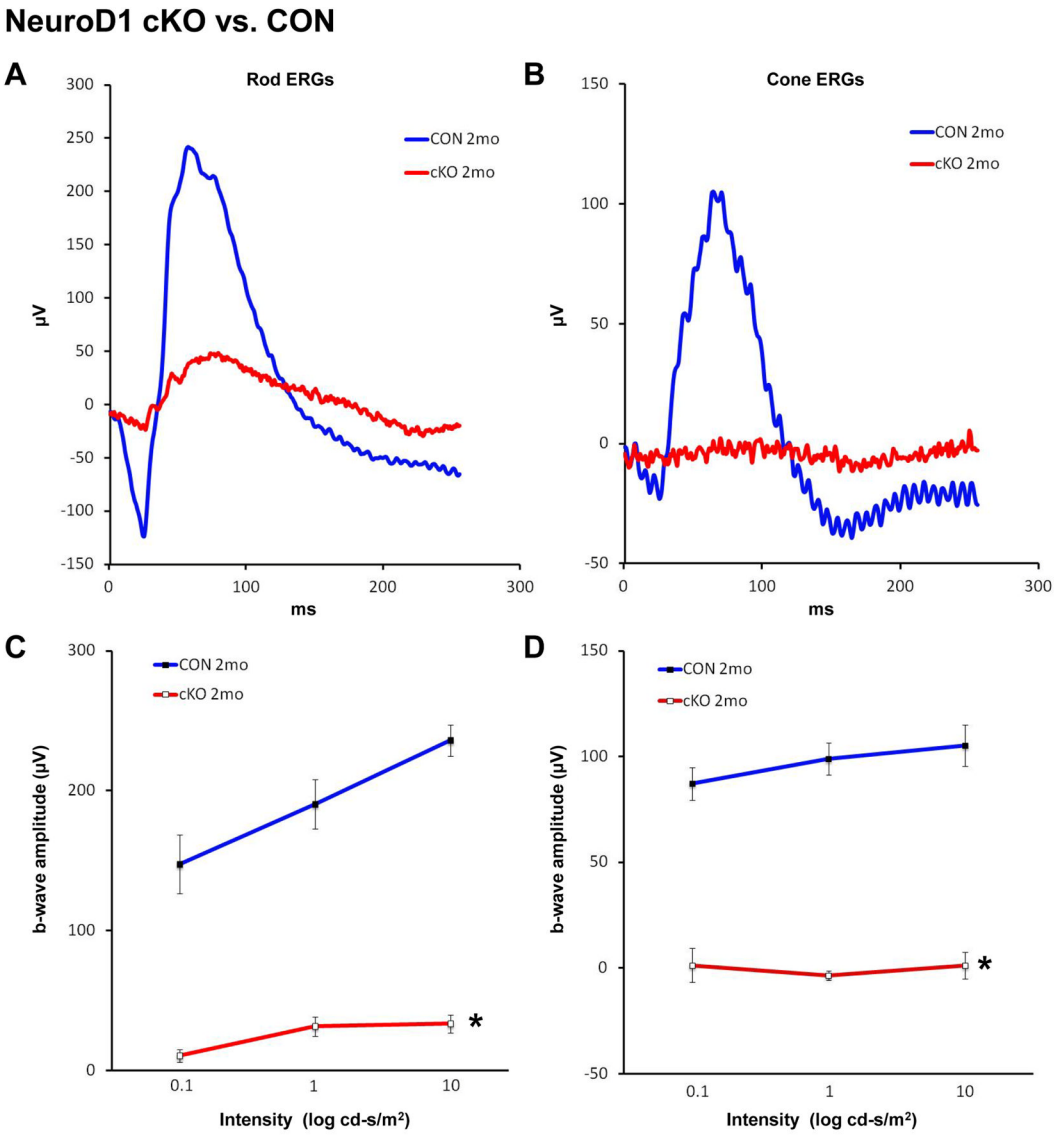

Figure 6. Electroretinograms from *NeuroD1* cKO mice compared to controls at two and four months of age

(A and B) *NeuroD1* cKO animals are nearly blind by two months of age based on rod and cone-driven electroretinogram responses. (C and D) The average rod and cone-driven b-wave amplitudes, respectively, at different light intensities for cKO and control animals at two months of age. Statistically significant reduction in rod and cone amplitudes at the highest intensity measured: *p<0.001. See Materials and Methods for further details.

NIH-PA Author Manuscript
NIH-PA Author Manuscript
NIH-PA Author Manuscript

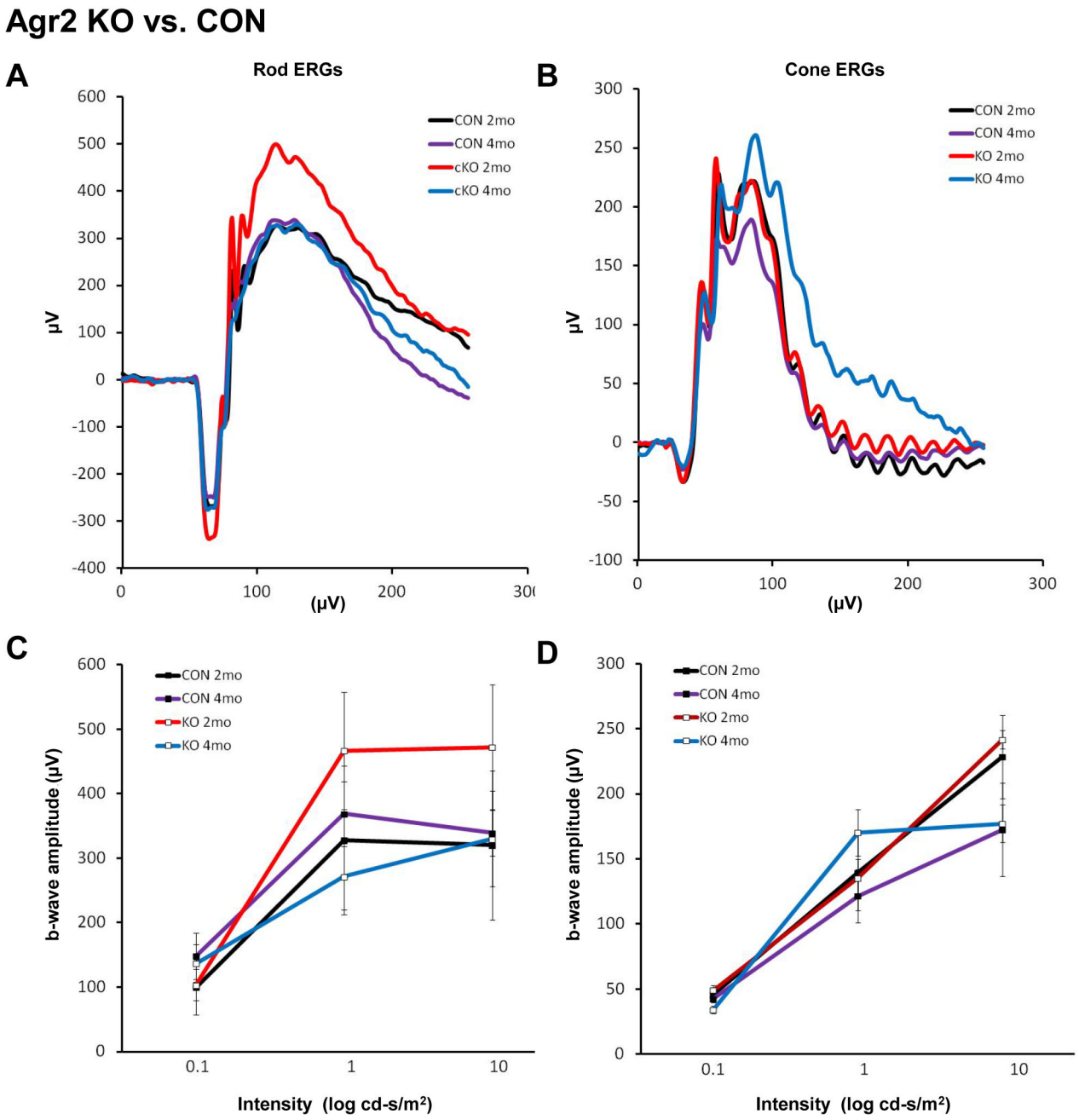

Figure 7. Electroretinograms from Agr2 KO mice compared to controls at two and four months of age

(A and B) In contrast to the *NeuroD1* cKO mice, *Agr2* KO animals do not show altered rod- or cone-driven electroretinograms at either two or four months of age. (C and D) Average rod and cone-driven B-wave amplitudes, respectively, for KO and control animals at two and four months of age. See Materials and Methods for further details.

NIH-PA Author Manuscript
NIH-PA Author Manuscript
NIH-PA Author Manuscript

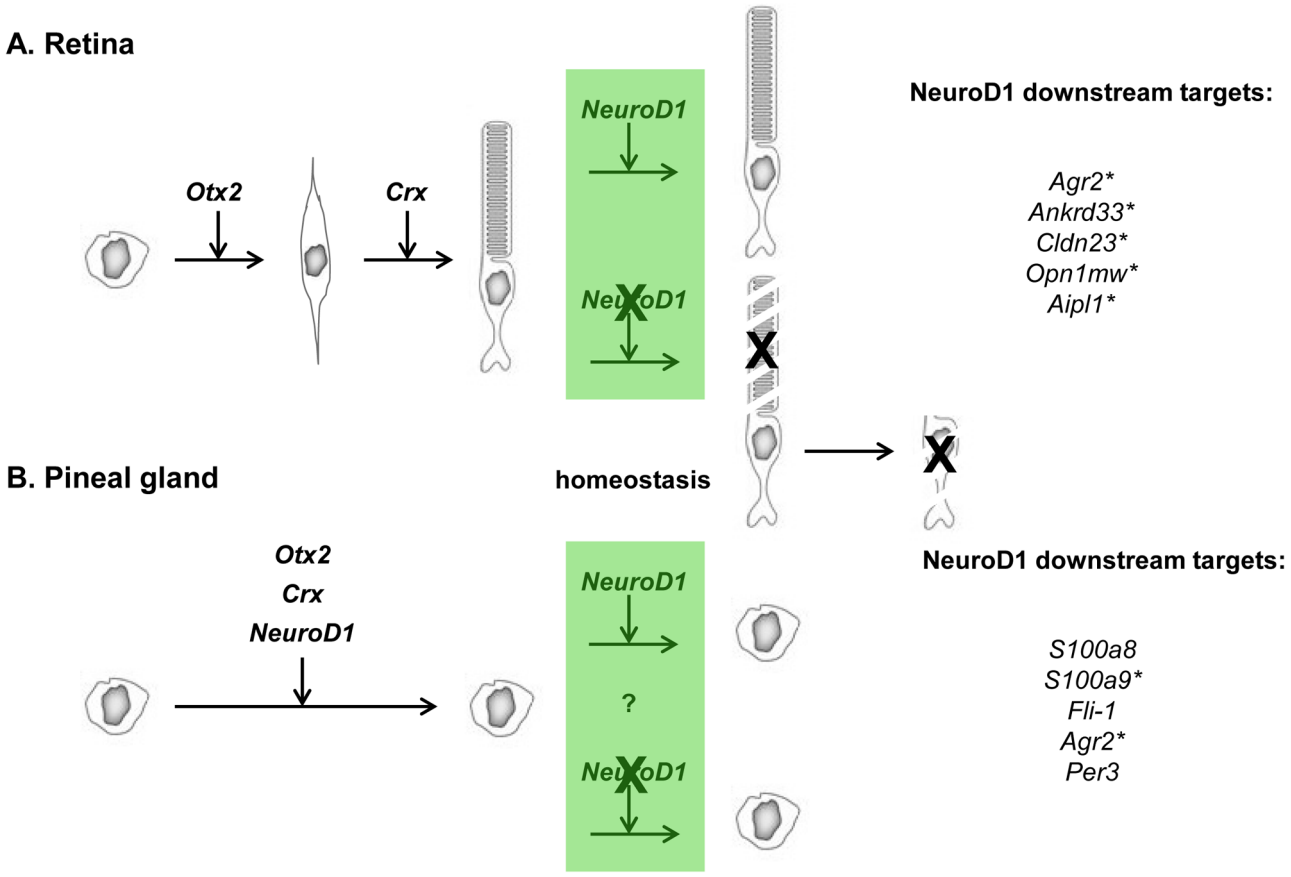

Figure 8. Schematic diagram illustrating NeuroD1 and its downstream targets in the photoreceptor and pinealocyte lineages

(A) Photoreceptor progenitors express *Otx2* and *Crx*. Differentiated photoreceptors express *NeuroD1* required for photoreceptor survival through a network of downstream targets including: *Agr2*, *Ankrd33*, *Cldn23*, *Opn1mw*, and *Aipl1*. (B) Pinealocyte progenitors express *Otx2* and *Crx*. Differentiated pinealocytes express *NeuroD1* which may play a role in maintenance of pinealocytes through a network of downstream targets including: *S100a8*, *S100a9*, *Agr2*, *Fli-1*, and *Per3*. Asterisks denote genes with promoters containing putative active *NeuroD1/E47* binding sites. The five most strongly down-regulated genes in both the retina and pineal gland are illustrated.

NIH-PA Author Manuscript NIH-PA Author Manuscript NIH-PA Author Manuscript

J Neurochem. Author manuscript; available in PMC 2013 October 01.

Table 1

Primers for genotyping and quantitative real-time PCR analysis.

Target	Sense-primer	Antisense-primer	Amplicon size (bp)	Accession number
Genotyping				
NeuroD1loxP	5′-GTTTTTGTGAGTTGGGAGTG-3′	5′-TGACAGAGCCCAGATGTA-3′	1011	-
NeuroD1wt	5′-GTTTTTGTGAGTTGGGAGTG-3′	5′-TGACAGAGCCCAGATGTA-3′	845	NM_010894
Cre	5′-ATGCTTCTGTCCGTTTGCCG-3′	5′-CCTGTTTTGCACGTTCACCG-3′	271	-
Agr2flox	5′-ACCTACATGGCCTTCCTTCC-3′	5′-ACCATCAAGGGTCTGTTGCT-3′	374	-
Agr2wt	5′-TATCCAGGCTCAGCAGGTTT-3′	5′-ACCATCAAGGGTCTGTTGCT-3′	267	NM_011783
qRT-PCR				
A2m	5′-ATTCACATCAAGCTGCATCTCATACT-3	5′-CTGTGAGAATTCAGTCAACAGCTAGA-3′	112	NM_175628
Agr2	5′-GGTCTACAAACACAATTCTGGGGAC-3′	5′-CAGAAATTGGCAGAGCAGTTTGTTC-3′	106	NM_011783
Aipl1	5′-CACCTCGTAGTACTCCTCCTTCTTC-3′	5′-GGAGAAGCCCTGGGAGGTTGA-3′	106	NM_053245
Ankrd33	5′-TTCCCGTCTTTGTCTTGCTGG-3′	5′-ATGGAGACCCTAGAGTCCCAG-3′	122	NM_144790
Cldn23	5′-GGAACAGGACAGTGTAGCATCG-3′	5′-ACTCCTATTTATATTTCTCTGTGCATATATAGT-3′	118	NM_027998
Dsp	5′-GAGTGATTTCGGTTTTGGTGACTG-3′	5′-TGCAGTCCCAGTTCACCGATG-3′	102	NM_023842
Edn2	5′-CTCTGGCAGTGTTAAGGCACAGA-3′	5′-GAGACCCCTATGCCTATCTCCTG-3′	122	NM_007902
Fli-1	5′-CTCAAAAATAATCCTTCTTTGTACTGGTGAC-3′	5′-GTGCAAAAAAAAAAGAAAATGTCCTGTTGT-3′	107	NM_008026
Gapdh	5′-CTGGAGAAACCTGCCAAGTA-3′	5′-TGTTGCTGTAGCCGTATTCA-3′	107	NM_008084
Gfap	5′-TCTGGTGAGCCTGTAATTGGGAC-3′	5′-TTCTCCAACCTCCAGATCCGAG-3′	115	NM_010277
lgl-V1	5′-GCCTTGTTAGTCTCGAGCTCTTCA-3′	5′-TAGTAGTGGCATTCGGGTGTTCG-3′	120	ENSMUST00000103741
NeuroD1	5′-CGCAGAAGGCAAGGTGTC-3′	5′-TTTGGTCATGTTTCCACTTCC-3′	90	NM_010894
Opn1mw	5′-AAAGGGACCTTTGGTGCTGTT-3′	5′-CCAAAGGCTTACAGGTGAACAGAC-3′	100	NM_008106
Opn1sw	5′-AGAAAGACATGGGTTTAGGGTACTATGA-3′	5′-GGAATACAGTAATTCTTAAAGAGGCCCAT-3′	101	NM_007538
Per3	5′-TAGCAGAGGTGAGACGTGGTAAAGGA-3′	5′-TATTTCCTTGCCTTTGTCCACACC-3′	112	NM_011067
Prlr	5′-AAAGGACCAAGATATAGCTGTCTCTTG-3′	5′-CCTTGGGTATTTTCTCTAGCTCCT-3′	118	NM_011164
Prtg	5′-GGAAGATAGGTCCGTGTTCTTGC-3′	5′-TCTCTGTGAGGTGGCTGCAAG-3′	102	NM_175485
Rho	5′-GGTCACCATCTCTCTATACTGCCTC-3′	5′-AAAGACTAGACTGTGTGGGGACA-3′	109	NM_145383
S100a8	5′-ATGATGACTTTATTCTGTAGACATATCCAGG-3′	5′-GTGATAAAAGTGGGTGTGGCATCT-3′	105	NM_013650
S100a9	5′-CTTTCTTCATAAAGGTTGCCAACTGT-3′	5′-CGACACCTTCCATCAATACTCTAGG-3′	107	NM_009114
Tal2	5′-GCATGAATTTGGGCTGAATTAAAAGAGTCA-3′	5′-ATGAACTGGACTGCATGGTTTTCTT-3′	110	NM_009317

NIH-PA Author Manuscript

NIH-PA Author Manuscript

NIH-PA Author Manuscript

Table 2

Differentially expressed genes in two-month-old *NeuroD1* cKO retina and pineal gland

(A) qRT-PCR validation of the ten most differentially expressed genes in the *NeuroD1* cKO retina, including genes linked to transcription, phototransduction and protein folding. (B) qRT-PCR validation of the ten most differentially expressed genes in the *NeuroD1* cKO pineal gland, including genes linked to transcription and calcium signaling. See Materials and Methods for further details.

Gene Symbol	Gene Title	Affymetrix Fold Change	qRT-PCR Fold Change	GO Biological Process Description
A. Retina: Differentially expressed genes in cKO vs CON				
NeuroD1	Neurogenic differentiation 1 transcription factor	−14.6	−26.9	Transcription activator activity, Photoreceptor cell development
Agr2	Anterior gradient homolog 2 (Xenopus laevis)	−7.9	−101.9	Protein binding
Ankrd33	Ankyrin repeat domain 33; Panky	−7.8	−9.9	Transcriptional cofactor
Cldn23	Claudin 23	−7.3	−37.2	Calcium-independent cell-cell adhesion
Opn1mw	Opsin 1 (cone pigments), medium-wave-sensitive	−4.4	−8.6	Phototransduction
Aipl1	Aryl hydrocarbon receptor interacting protein-like 1	−3.0	−3.8	Phototransduction
Gfap	Glial fibrillary acidic protein	5.4	7.0	Structural constituent of cytoskeleton
Prtg	Protogenin	5.7	6.4	Multicellular organismal development
Edn2	Endothelin-2	7.4	9.9	Cell surface receptor linked signaling pathway
A2m	Alpha-2-macroglobulin	7.6	13.3	Response to glucocorticoid stimulus
Tal2	T-cell acute lymphocytic leukemia protein 2	11.8	132.8	Transcription regulator activity, DNA binding
B. Pineal: Differentially expressed genes in cKO vs CON				
NeuroD1	Neurogenic differentiation 1 transcription factor	−47.8	−196.5	Transcription activator activity, Photoreceptor cell development
S100a8	S100 calcium-binding protein A8 (calgranulin A)	−3.3	−4.4	Chemotaxis, calcium binding, inflammatory response
S100a9	S100 calcium-binding protein A9 (calgranulin B)	−3.1	−4.3	Actin cytoskeleton reorganization, calcium binding
Fli-1	Friend leukemia integration 1 transcription factor	−2.5	−3.4	Regulation of transcription, DNA-dependent
Agr2	Anterior gradient homolog 2 (Xenopus laevis)	−2.2	−3.4	Protein binding
Per3	Period 3	−2.1	−1.6	Regulation of transcription, DNA-dependent, rhythmic process
Dsp	Desmoplakin	2.2	2.8	Beta catenin signaling
Prlr	Prolactin receptor	2.2	2.6	Cytokine receptor degradation signaling

NIH-PA Author Manuscript

NIH-PA Author Manuscript

NIH-PA Author Manuscript

Gene Symbol	Gene Title	Affymetrix Fold Change	qRT-PCR Fold Change	GO Biological Process Description
Igl-V1	Immunoglobulin lambda chain, variable 1	9.1	7.2	B cell signaling, Immune response

NIH-PA Author Manuscript

NIH-PA Author Manuscript

NIH-PA Author Manuscript

Table 3

Genes exhibiting a night/day rhythm in the control and/or *NeuroD1* cKO retina and pineal gland

The table shows genes that are rhythmic in (A) This section of the table depicts three categories of gene groups found in the control and *NeuroD1* cKO retina: Genes that are rhythmic in both the control and cKO retina; genes that become arrhythmic in the cKO retina; and genes that gain rhythmicity in the cKO retina. (B) This section of the table depicts three categories of gene groups found in the control and cKO pineal gland: Genes that are rhythmic in both the control and cKO pineal gland; genes that become arrhythmic in the cKO pineal gland; and genes that gain rhythmicity in the cKO pineal gland. See Materials and Methods for further details.

Night/Day Ratio	Rhythmic in CON and cKO	Rhythmic in CON	Rhythmic in cKO
A. Retina: Genes exhibiting a night/day rhythm in CON and cKO			
2 to 4	Irf7, Pgbd1, Nr4a1, Sik2, Zdhhc5	Casz1, Aqp1, Hspa1b, Thbs1, Drd4	Gsta3, Trpm1, Atp1a2, Slc13a4, Fbin1, Rorb, Gpx3
1/2 to 1/4	Col19a1, Dynlarb2, Phospho2, Glmn, Taf4b	Dnase2b, Krt6b, Krt15, Emp1, Sgcg, Crh, Lenep, Flad1, Pgam2, Eif2s3y, Slamf1, Kdm5d, Dio2, Dleu7, Ccl9, Rprd2, Ucma	Akap5, Tmem116, Ly75, Adcy1
B. Pineal: Genes exhibiting a night/day rhythm in CON and cKO			
8 to 12	Gng4, E2f8, Aanat, Cpm	-	-
4 to 8	Stc2, Kcnc1, Gulo, Piwil4, Pgbd1, Tbc1d1, Ifng, Dclk1, Ednrb,	Frmd1	Slc6a5, St8sia2, Grm4,
2 to 4	Gls2, Lrfn2, Kif5c, Cckbr, Rftn1, Adra1b	Cyth3, Ednra, Plekho2, Odc1, Rimkla	Dlk1, Nr4a1, Ppa2, Pparg
1/2 to 1/4	Hspa12a, Dpp10, Ppp2r2b, Cntn4, Wdr17, Nr1d1, Gabra1, Nrxn3	Ifi202b, Ifi203, Tmem90a, Mtap2	Caccnb2, Adcy1, Bai3, Opn1sw, Isl2, Fam19a3, Ush2a
1/4 to 1/8	Clca3		

NIH-PA Author Manuscript
NIH-PA Author Manuscript
NIH-PA Author Manuscript

Table 4

The two stages of photoreceptor degeneration phenotype observed in the *NeuroD1* cKO retina

At two months of age the absence of *NeuroD1* leads to selective degeneration of the outer segments and reduced or absent ERG responses. In turn, this loss of outer segments and associated changes may lead to the disappearance of the photoreceptor cell bodies, as observed by four months of age. The ONL, which contains both the cone and rod photoreceptor cell bodies, is absent by four months of age.

Photoreceptors	2 months	4 months
Rods		
Morphology	Outer segments shortened and disorganized, cell bodies present	ONL absent
Rho protein	Rho partially mislocalized to inner segment; reduced 95%	N/A
Rho mRNA	Reduced 40%	N/A
ERG	Significantly reduced	N/D
M-cones		
Morphology	Nearly absent	ONL absent
M-Opsin protein	Nearly absent	N/A
M-Opsin mRNA	Reduced 80%	N/A
ERG	N/D	N/D
S-cones		
Morphology	Outer segments disorganized, cell bodies present	ONL absent
S-Opsin protein	S-opsin mislocalized to cell membrane and synapse	N/A
S-Opsin mRNA	No change	N/A
ERG	N/D	N/D

ONL, outer nuclear layer; N/D, Not Detected; N/A, Not Analyzed. See Materials and Methods for further details.